Published in Journal of the American Chemical Society (JACS) 134, issue 2, pp. 754–757, 2012,
which should be used for any reference to this work

Organometallic Cages as Vehicles for Intracellular Release of Photosensitizers

Frédéric Schmitt,[†] Julien Freudenreich,[‡] Nicolas P. E. Barry,[‡] Lucienne Juillerat-Jeanneret,[†] Georg Süss-Fink,[‡] and Bruno Therrien*[,‡]

[†]Institut Universitaire de Pathologie, Centre Hospitalier Universitaire Vaudois, Bugnon 25, CH-1011 Lausanne, Switzerland

[‡]Institute of Chemistry, University of Neuchâtel, Avenue de Bellevaux 51, CH-2000 Neuchâtel, Switzerland

ABSTRACT: Water-soluble metalla-cages were used to deliver hydrophobic porphin molecules to cancer cells. After internalization, the photosensitizer was photoactivated, significantly increasing the cytotoxicity in cells. During the transport, the photosensitizer remains nonreactive to light, offering a new strategy to tackle overall photosensitization, a limitation often encountered in photodynamic therapy.

In recent years, the use of large vehicles to carry photosensitizers to cancer cells has attracted much interest.[1] Photosensitizers such as porphyrins and phthalocyanines are in general poorly water-soluble, unless highly substituted with hydrophilic groups.[2] Therefore, encapsulation of the photosensitizer within the hydrophobic cavity of water-soluble carriers provides an elegant strategy to transport photosensitizers in aqueous media, a necessity for biological applications. Moreover, most photosensitizers show poor selectivity to diseased cells and consequently generate an overall photosensitization of the entire body. Thus, spatial-controlled release of the photosensitizer remains one of the main challenges in photodynamic therapy.[3]

Recently, water-soluble arene ruthenium metalla-cages have been used to deliver hydrophobic molecules to cancer cells.[4] In an extension to this work, we have now encapsulated porphin, a well-known lipophilic photosensitizer,[5] in two cationic arene ruthenium metalla-cages (Figure 1). In the hexanuclear metalla-prism, $[Ru_6(\eta^6\text{-}p\text{-}Pr^iC_6H_4Me)_6(tpt)_2(dobq)_3]^{6+}$ ($[\mathbf{1}]^{6+}$; tpt = 2,4,6-tris(4-pyridyl)-1,3,5-triazine; dobq = 2,5-dioxido-1,4-benzoquinonato), porphin is trapped in the cavity of $[\mathbf{1}]^{6+}$, while in the larger octanuclear metalla-cube

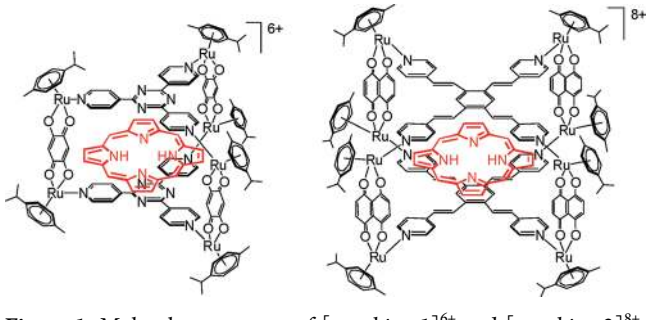

Figure 1. Molecular structures of [porphin⊂**1**]$^{6+}$ and [porphin⊂**2**]$^{8+}$.

$[Ru_8(\eta^6\text{-}p\text{-}Pr^iC_6H_4Me)_8(tpvb)_2(donq)_4]^{8+}$ ($[\mathbf{2}]^{8+}$; tpvb = 1,2,4,5-tetrakis{2-(4-pyridyl)vinyl}benzene; donq = 5,8-dioxido-1,4-naphthoquinonato), porphin is reversibly encapsulated and can be released without rupture of the cage compound. The antiproliferative activity and the phototoxicity of the empty cages and the porphin⊂cage systems have been evaluated on human cancer cell lines from different phenotypes. Moreover, stability of the cages, uptake of the host–guest systems, and release of porphin after internalization in the cells have been studied by fluorescence spectroscopy.

Synthesis of the empty metalla-prism $[\mathbf{1}]^{6+}$ has been reported previously.[4] However, synthesis of the carceplex [porphin⊂**1**]$^{6+}$ is new and requires the addition of porphin during the formation of $[\mathbf{1}]^{6+}$ (see Supporting Information (SI)). The encapsulation of porphin in $[\mathbf{1}]^{6+}$ is easily monitored by ^{1}H NMR spectroscopy (Figure 2). Indeed, the signals associated with the protons of the porphin molecule are shifted upfield due to the encapsulation. Moreover, diffusion-ordered NMR spectroscopy (DOSY)[6] clearly demonstrates that the porphin molecule is trapped in the hydrophobic cavity of $[\mathbf{1}]^{6+}$, as illustrated in Figure 2. The carceplex [porphin⊂**1**]$^{6+}$ is isolated as the triflate salt.

Synthesis of the metalla-cube $[\mathbf{2}]^{8+}$ follows the same strategy using 4 equiv of $[Ru_2(\eta^6\text{-}p\text{-}Pr^iC_6H_4Me)_2(donq)Cl_2]$[7] and 2 equiv of tpvb[8] in methanol at reflux for 24 h (SI). Likewise, $[porphin⊂\mathbf{2}][CF_3SO_3]_8$ is prepared by adding 1 equiv of porphin during the formation of $[\mathbf{2}]^{8+}$. The empty cage and the host–guest system have been fully characterized by ^{1}H, ^{13}C, and DOSY NMR spectroscopy, as well as by ESI-MS and elemental analysis. The encapsulation of porphin in the cavity of $[\mathbf{2}]^{8+}$ was confirmed by DOSY measurements (Figure 2). As compared to [porphin⊂**1**]$^{6+}$, the proton signals of the encapsulated porphin molecule in $[\mathbf{2}]^{8+}$ are broad with a similar upfield shift, but as expected for a porphin⊂cage system they are all diffusing with the proton signals of the cage. The broadness of the signals is due to the large cavity size of $[\mathbf{2}]^{8+}$, in which porphin is free to move. Indeed, Chem3D models of both[9] [porphin⊂**1**]$^{6+}$ and [porphin⊂**2**]$^{8+}$ systems give clear pictures of the porphin environment in the cavities of $[\mathbf{1}]^{6+}$ and $[\mathbf{2}]^{8+}$ (Figure 3).

Spectroscopic measurements were realized on porphin, the empty cages as well as the porphin⊂cage systems. UV–vis

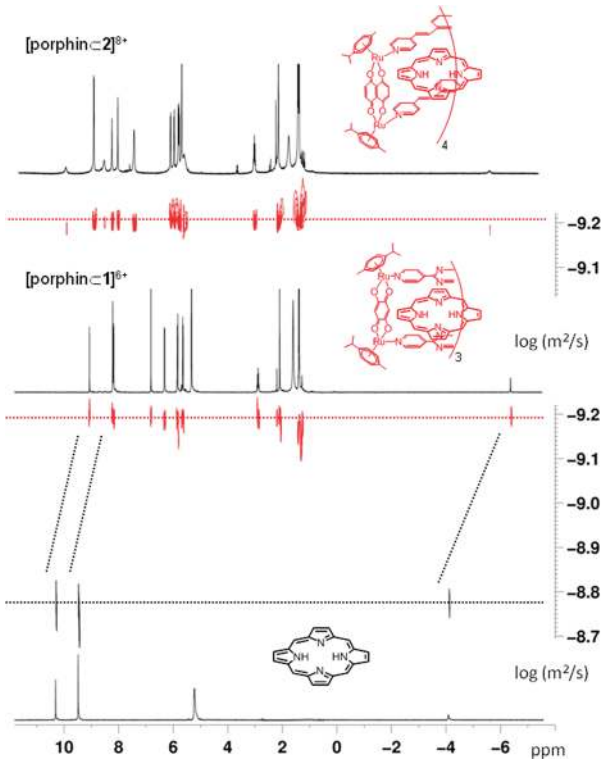

Figure 2. ^{1}H NMR (CD_2Cl_2, 23 °C) and DOSY spectra of porphin, [porphin⊂**1**][CF_3SO_3]$_6$, and [porphin⊂**2**][CF_3SO_3]$_8$.

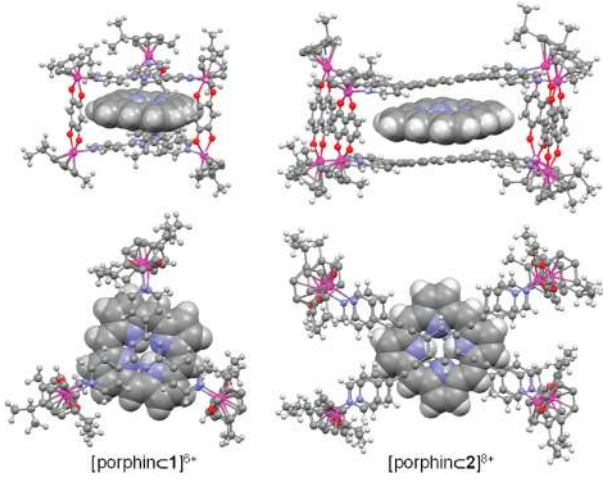

Figure 3. Chem3D models of the metalla-cages [porphin⊂**1**]$^{6+}$ and [porphin⊂**2**]$^{8+}$: side and top views.

absorption spectra reveal hypochromism of the characteristic porphin bands when trapped inside both cages (Figure S1), while the porphin fluorescence intensity almost vanishes upon encapsulation (see Figure 4). The strong hypochromism of the fluorescence is a useful phenomenon to study the uptake and stability of the systems as well as to follow the release of the guest by the cage compounds after internalization by the cells.[10] In addition, the ability of porphin, the empty cages, and the porphin⊂cage compounds to generate reactive oxygen species has been evaluated. All complexes [**1**][CF_3SO_3]$_6$, [**2**]-[CF_3SO_3]$_8$, [porphin⊂**1**][CF_3SO_3]$_6$, and [porphin⊂**2**]-[CF_3SO_3]$_8$ show no production of singlet oxygen in ethanol/DMSO as opposed to porphin, which possesses after excitation at 414 nm a singlet oxygen quantum yield of 97% (Table S1).

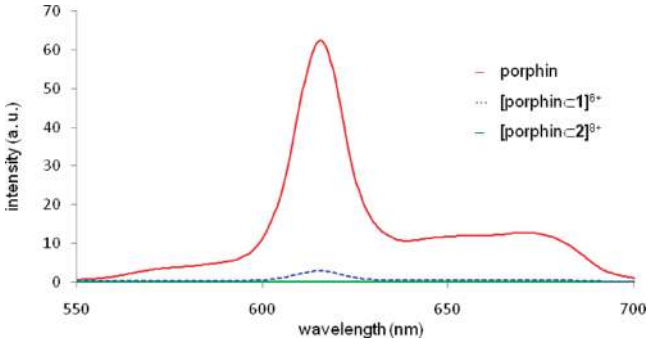

Figure 4. Fluorescence spectra of porphin and porphin⊂cage systems (isopropanol/dmso, 10^{-4} M, excitation 405 nm).

Consequently, empty and porphin⊂cage systems can be considered harmless in term of phototoxicity; only after release of porphin is photoactivity regained.

The stability of the porphin⊂cage systems has been evaluated under various biological conditions (see SI). All complexes are stable at physiological pH from 6 to 8 at 37 °C. In the presence of oxidative (H_2O_2) or reductive (dithiothreitol) derivatives, no degradation of the host−guest systems is observed. Similarly, when exposed to complete culture medium, the porphin⊂cage systems remain intact.

The uptake and release of porphin after internalization of the host−guest systems have been studied for various human cancer cells, Me300, A2780, A2780cisR, HeLa, and A549 (Table 1). The antiproliferative activity of the complexes in the

Table 1. Cytotoxicity of Porphin⊂Cage Systems for Various Human Cancer Cells after 72 h Incubation in the Dark

	IC_{50} (μM)	
cells	[porphin⊂**1**]$^{6+}$	[porphin⊂**2**]$^{8+}$
Me300	5.7 ± 0.9	5.0 ± 0.1
A2780	6.0 ± 0.8	12.0 ± 0.5
A2780cisR	5.2 ± 0.9	6.2 ± 1.7
HeLa	9.5 ± 1.3	12.5 ± 3.1
A549	8.5 ± 1.7	11.2 ± 5.0

dark was evaluated, demonstrating that the empty cages and porphin⊂cage systems present moderate cytotoxicities with comparable values in the cell lines tested. All IC_{50} values are comprised in the range 5−12 μM (Table 1), and no significant differences were found between the empty and porphin⊂cage systems. Moreover, despite the presence of eight ruthenium atoms per metalla-cage in [**2**]$^{8+}$, as opposed to only six in [**1**]$^{6+}$, [porphin⊂**2**]$^{8+}$ is slightly less cytotoxic than [porphin⊂**1**]$^{6+}$.

Interestingly, the porphin fluorescence could be detected intracellularly during the incubation of cells with the porphin⊂cage systems. A stronger signal for [porphin⊂**2**]$^{8+}$ than [porphin⊂**1**]$^{6+}$ in all cell lines was observed, suggesting a higher porphin release inside the cells (Figure 5). The differences in fluorescence after 72 h incubation can be correlated to the nature of the porphin⊂cage systems. Indeed, as emphasized in Figure 3, the release of porphin requires two different mechanisms depending on the cages: rupture of the cage in [porphin⊂**1**]$^{6+}$, while in [porphin⊂**2**]$^{8+}$ the porphin molecule can diffuse through an aperture without breakage of the cage.

The uptake of the porphin⊂cage systems by cells was further visualized by fluorescence microscopy. Cells incubated with

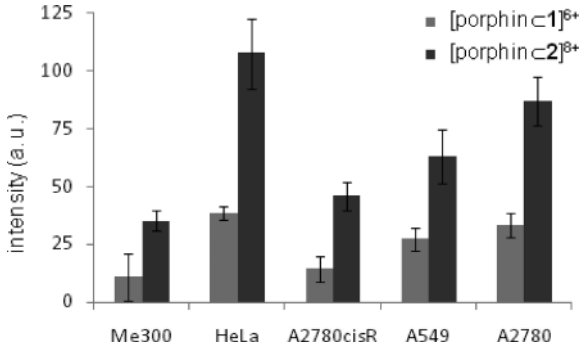

Figure 5. Fluorescence of porphin detected in cancer cells after 72 h incubation (5 μM porphin⊂cage systems).

$[porphin⊂\mathbf{1}]^{6+}$ did not present enough fluorescence to be detected, while incubation with $[porphin⊂\mathbf{2}]^{8+}$ revealed strong red and blue fluorescence spots corresponding to porphin molecules and empty cages, respectively (Figure 6). These

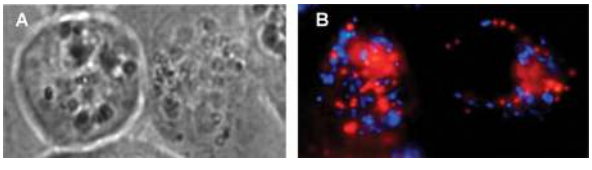

Figure 6. Fluorescence microscopy of HeLa cells incubated with $[porphin⊂\mathbf{2}]^{8+}$ (2 μM, 20 h): (A) white light and (B) fluorescence.

findings confirm the intracellular release of porphin from the cage and also indicate that both the cage and porphin are located in different compartments of the cell and not in the nucleus.

The photodynamic efficiency of both porphin⊂cage systems was evaluated in HeLa cells at 0.5 μM concentration (~20 times below the IC_{50} concentration, 20 h incubation). Excellent phototoxicities were found for both cages, confirming the release of porphin from the cage (Figure 7). Moreover,

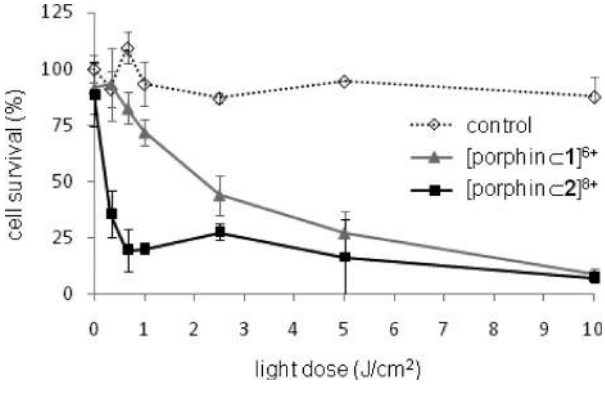

Figure 7. Photodynamic activity of porphin⊂cage systems (0,5 μM, 20 h, 488 nm irradiation) in HeLa cancer cells (control being cells irradiated without compound).

$[porphin⊂\mathbf{2}]^{8+}$ (0.2 J/cm^2) was 10 times more photoactive than $[porphin⊂\mathbf{1}]^{6+}$ (2.1 J/cm^2). This result is in complete agreement with intracellular measurements of porphin fluorescence and singlet oxygen quantum yield, linking the release of porphin with photoefficiency.

In conclusion, we have demonstrated that the metalla-cages were able to carry and deliver intracellularly photosensitizers following uptake by cells. The release of porphin is higher for the larger cubic cage as compared to the smaller prismatic cage. These systems display hypochromism properties toward the photosensitizer loaded inside the cavity of the cage, resulting in the absence of phototoxic effect outside of cells. This ability defines our cages as very safe and powerful tools for new photodynamic strategies that may not induce overall photosensitization in patients and therefore allow better efficiency in photodynamic treatment.

■ ASSOCIATED CONTENT

Ⓢ Supporting Information

Experimental details, UV−vis spectra, and singlet oxygen quantum yields. This material is available free of charge via the Internet at http://pubs.acs.org.

■ AUTHOR INFORMATION

Corresponding Author

bruno.therrien@unine.ch

■ ACKNOWLEDGMENTS

We thank G. Wagnières (LPAS, EPFL, Lausanne) for providing the PDT lamp and for help in the PDT experiments. We also thank C. Frochot (LRGP-CNRS, Nancy, France) for assistance in determining the singlet oxygen quantum yields and Johnson Matthey Research Centre for a generous loan of $RuCl_3$ hydrate.

■ REFERENCES

(1) (a) Gilyazova, D. G.; Rosenkranz, A. A.; Gulak, P. V.; Lunin, V. G.; Sergienko, O. V.; Khramtsov, Y. V.; Timofeyev, K. N.; Grin, M. A.; Mironov, A. F.; Rubin, A. B.; Georgiev, G. P.; Sobolev, A. S. *Cancer Res.* **2006**, *66*, 10534. (b) Ngweniform, P.; Abbineni, G.; Cao, B.; Mao, C. *Small* **2009**, *5*, 1963. (c) Yan, F.; Zhang, Y.; Kim, K. S.; Yuan, H.-K.; Vo-Dinh, T. *Photochem. Photobiol.* **2010**, *86*, 662. (d) Brasch, M.; de la Escosura, A.; Ma, Y.; Uetrecht, C.; Heck, A. J. R.; Torres, T.; Cornelissen, J. J. L. M. *J. Am. Chem. Soc.* **2011**, *133*, 6878. (e) van Hell, A. J.; Fretz, M. M.; Crommelin, D. J. A.; Hennink, W. E.; Mastrobattista, E. *J. Controlled Release* **2010**, *141*, 347. (f) Schmitt, F.; Lagopoulos, L.; Käuper, P.; Rossi, N.; Busso, N.; Barge, J.; Wagnières, G.; Laue, C.; Wandrey, C.; Juillerat-Jeanneret, L. *J. Controlled Release* **2010**, *144*, 242.

(2) (a) Moreira, L. M.; dos Santos, F. V.; Lyon, J. P.; Maftoum-Costa, M.; Pacheco-Soares, C.; Soares da Silva, N. *Aust. J. Chem.* **2008**, *61*, 741. (b) Wainwright, M. *Anti-Cancer Agents Med. Chem.* **2008**, *8*, 280. (c) Canlica, M.; Nyokong, T. *Dalton Trans.* **2011**, *40*, 1497. (d) Vedachalam, S.; Choi, B.-H.; Kumar Pasunooti, K.; Mei Ching, K.; Lee, K.; Sup Yoon, H.; Liu, X.-W. *Med. Chem. Commun.* **2011**, *2*, 371. (e) Lau, J. T. F.; Lo, P.-C.; Fong, W.-P.; Ng, D. K. P. *Chem. Eur. J.* **2011**, *17*, 7569.

(3) (a) Lane, N. *Sci. Am.* **2008**, *18*, 80. (b) Zeisser-Labouèbe, M.; Mattiuzzo, M.; Lange, N.; Gurny, R.; Delie, F. *J. Drug Target.* **2009**, *17*, 619. (c) O'Connor, A. E.; Gallagher, W. M.; Byrne, A. T. *Photochem. Photobiol.* **2009**, *85*, 1053. (d) Ethirajan, M.; Chen, Y.; Joshi, P.; Pandey, R. K. *Chem. Soc. Rev.* **2011**, *40*, 340.

(4) (a) Therrien, B.; Süss-Fink, G.; Govindaswamy, P.; Renfrew, A. K.; Dyson, P. J. *Angew. Chem., Int. Ed.* **2008**, *47*, 3773. (b) Mattsson, J.; Zava, O.; Renfrew, A. K.; Sei, Y.; Yamaguchi, K.; Dyson, P. J.; Therrien, B. *Dalton Trans.* **2010**, *39*, 8248. (c) Vajpayee, V.; Yang, Y. J.; Kang, S. C.; Kim, H.; Kim, I. S.; Wang, M.; Stang, P. J.; Chi, K.-W. *Chem. Commun.* **2011**, *47*, 5184.

(5) Berg, K.; Selbo, P. K.; Weyergang, A.; Dietze, A.; Prasmickaite, L.; Bonsted, A.; Engesaeter, B. Ø.; Angell-Petersen, E.; Warloe, T.; Frandsen, N.; Høgset, A. *J. Microsc.* **2005**, *218*, 133.

(6) (a) Wu, D.; Chen, A.; Johnson, C. S. Jr. *J. Magn. Reson. A* **1995**, *115*, 123. (b) Johnson, C. S. Jr. *Prog. Nucl. Magn. Reson. Spectrosc.* **1999**, *34*, 203. (c) Ajami, D.; Rebek, J. Jr. *Angew. Chem., Int. Ed.* **2007**,

46, 9283. (d) Lemonnier, J.-F.; Floquet, S.; Kachmar, A.; Rohmer, M.-M.; Bénard, M.; Marrot, J.; Terazzi, E.; Piguet, C.; Cadot, E. *Dalton Trans.* **2007**, 3043. (e) Barry, N. P. E; Furrer, J.; Freudenreich, J.; Süss-Fink, G.; Therrien, B. *Eur. J. Inorg. Chem.* **2010**, 725. (f) Barry, N. P. E; Furrer, J.; Therrien, B. *Helv. Chim. Acta* **2010**, *93*, 1313.

(7) Barry, N. P. E; Therrien, B. *Eur. J. Inorg. Chem.* **2009**, 4695.

(8) Amoroso, A. J.; Cargill Thompson, A. M. W.; Maher, J. P.; McCleverty, J. A.; Ward, M. D. *Inorg. Chem.* **1995**, *34*, 4828.

(9) *Chem3D Pro 11.0 for PC*;CambridgeSoft: Cambridge, MA.

(10) (a) Zava, O.; Mattsson, J.; Therrien, B.; Dyson, P. J. *Chem. Eur. J.* **2010**, *16*, 1428. (b) Barry, N. P. E; Zava, O.; Dyson, P. J.; Therrien, B. *Chem. Eur. J.* **2011**, *17*, 9669.